






## RESEARCH ARTICLE

10.1029/2022JD038025

# Propagation and Characteristics of Hydrometeorological Drought Under Changing Climate in Irish Catchments

H. Meresa<sup>1</sup> , C. Murphy<sup>1</sup> , and S. E. Donegan<sup>1</sup> 

<sup>1</sup>Irish Climate Analysis and Research UnitS (ICARUS), Department of Geography, Maynooth University, Maynooth, Ireland

### Key Points:

- Changes in hydrometeorological drought characteristics under changing climate conditions were estimated; and the results indicate substantial drying during summer with associated increases in summer drought magnitude and frequency
- Increases in winter and spring precipitation result in a decrease in the frequency and magnitude of drought events outside summer and are critical for maintaining baseflow during summer. This also raises the risk of extreme droughts for a dry winter/spring
- The probability of drought propagation from meteorological to hydrological events increases for the 2050s but decreases for the end of century, highlighting the importance of increases in winter and spring precipitation to drought risk

### Supporting Information:

Supporting Information may be found in the online version of this article.

### Correspondence to:

H. Meresa,  
[hadush.meres@mu.ie](mailto:hadush.meres@mu.ie)

### Citation:

Meres, H., Murphy, C., & Donegan, S. E. (2023). Propagation and characteristics of hydrometeorological drought under changing climate in Irish catchments. *Journal of Geophysical Research: Atmospheres*, 128, e2022JD038025. <https://doi.org/10.1029/2022JD038025>

Received 14 OCT 2022

Accepted 22 APR 2023

**Abstract** Hydrometeorological droughts are complex hazards expressed through the relative deviation in water availability relative to long-term average conditions. The development and propagation of drought is governed by hydrological processes at different spatial scales including precipitation, evapotranspiration, overland flow, soil moisture, groundwater storage and discharge. Detailed investigation is thus required to evaluate associated linkages among various types of hydrometeorological drought to understand the likely impacts of climate change on drought characteristics (magnitude, frequency, duration and propagation). This study explores the impact of climate change on hydrometeorological drought for 10 Irish catchments, using standardized drought indices representing different components of the hydrological system. We employ 12 Global Climate Models from the Coupled Model Inter-comparison Project phase 6 (CMIP6), forced with SSP370 and bias corrected to catchment conditions to force a conceptual hydrological model to generate hydrological projections for each catchment. The results indicate substantial drying during summer with associated increases in summer drought magnitude and frequency. However, simulations show a wide range of change, especially for hydrological drought (discharge and baseflow). Only modest changes in the magnitude and frequency of hydrological drought events were found, with increases in winter and spring precipitation offsetting summer dryness. Similarly, the probability of meteorological drought propagating to hydrological events (Standardized Streamflow Index/Standardized Baseflow Index), shows modest increases under the climate change projections considered. Findings highlight that drought, especially during summer are a critical climate change risk for adaptation.

**Plain Language Summary** Climate change aggravates the impact of hydrometeorological droughts on water availability and distribution in Ireland. Rainfall, evaporation, overland flow, soil moisture, groundwater storage, and the size and strength of discharges are the main factors that cause drought extent and duration. Therefore, for the sustainable development of ecosystems and water resources in a country, it is a requirement to evaluate associated linkages among various types of hydrometeorological drought to understand the likely impacts of climate change on drought characteristics (magnitude) and propagation. This paper explores the impact of climate change on hydrometeorological drought for 10 Irish catchments. The findings indicate significant summer drying, as well as increases in the magnitude and frequency of summer droughts. The probability of meteorological drought propagating to hydrological events, shows modest increases under the climate change projections considered. Drought, particularly during the summer, is a critical climate change risk for adaptation, according to the findings.

## 1. Introduction

Hydrometeorological droughts are complex hazards expressed through the relative deviation in water availability relative to long-term average conditions. They are typically slow onset, propagating through the water cycle to affect different social, economic, and environmental sectors at different temporal and spatial scales (Ayantobo et al., 2017; Gaitán et al., 2020; Quevauviller & Gemmer, 2015). Furthermore, flash droughts with rapid onset propagate through different spatial-temporal scales, from atmospheric to surface conditions (Shah et al., 2022). Although drought is predominantly caused by a lack of precipitation, soil moisture and streamflow, other factors, like prolonged abstraction and rising atmospheric evaporative demand (AED), can affect drought incidence and propagation. Moreover, the development and propagation of drought is governed by hydrological processes at different spatial scales including precipitation, evapotranspiration, overland flow, soil moisture, groundwater storage and discharge (Ganguli et al., 2022; Sutanto & Van Lanen, 2022). Detailed investigation is thus required to evaluate associated linkages among various types of hydrometeorological drought to understand the likely impacts of climate change on drought characteristics (magnitude, frequency, duration and propagation) at the

© 2023. The Authors.

This is an open access article under the terms of the [Creative Commons Attribution-NonCommercial-NoDerivs License](https://creativecommons.org/licenses/by/4.0/), which permits use and distribution in any medium, provided the original work is properly cited, the use is non-commercial and no modifications or adaptations are made.

catchment scale (Mishra & Cherkauer, 2010). The impact of climate change on drought characteristics has been widely investigated, with the frequency and occurrence of meteorological drought expected to worsen due to increasing greenhouse gas concentrations in major world regions (IPCC, 2021). Recent extreme droughts have increased the urgency of understanding the impact of climate change on droughts. European drought in 2015 and 2018 (Falzoi et al., 2019; Ionita et al., 2017; Roudier et al., 2015; Stagge et al., 2015), in east Africa during 1984 and 2015 (Funk et al., 2019; Oguntunde et al., 2017), Australia in 2019 (Kirono et al., 2020) and the USA, particularly in California, have clearly demonstrated the pervasive impact of drought on water resources, ecology, biodiversity and agriculture (He et al., 2019; Mann & Gleick, 2015; Ullrich et al., 2018). In turn, many studies have examined the impact of climate change and variability on hydrometeorological droughts (Hanel et al., 2018; H. K. Meresa et al., 2016; C. Murphy et al., 2020; Noone et al., 2017; Oguntunde et al., 2017; Stagge et al., 2015). Besides the spatial differences, the main conclusion of these studies is an expected increase in meteorological drought with climate change. However, the impact of climate change on soil moisture deficits, runoff, and base-flow are less understood.

Hydrometeorological drought indices are widely used to investigate changes in drought characteristics. These indices are typically derived from single or multiple meteorological and/or hydrological variables, such as precipitation ( $P$ ), AED, streamflow/runoff ( $R$ ), and temperature ( $T$ ) (Mukherjee et al., 2018). Over recent decades >160 hydrometeorological drought indices have been developed to detect, monitor and characterize droughts (Niemeyer, 2008) with commonly applied examples including the Palmer Drought Severity Index (PDSI) (Palmer, 1965), the Standardized Precipitation Index (SPI) (McKee et al., 1993), the Standardized Precipitation Evapotranspiration Index (SPEI) (Vicente-Serrano, et al., 2020a), the Rainfall Anomaly Index (RAI), the Standardized Runoff Index (SRI) (Shukla & Wood, 2008), the Standardized Soil-Moisture Index (SSMI) (Hao & Aghakouchak, 2013), and the Reconnaissance Drought Index (RDI) (Tsakiris & Vangelis, 2005). Each has its own strengths and weaknesses and it is challenging to select a single standard method. For instance, SPI is widely applied and can detect drought conditions at different timescales, ranging from monthly to multi-annual (McKee et al., 1993). However, SPI is based on precipitation alone and fails to consider the role of temperature on drought events and frequencies (Reyniers et al., 2022) and may not be suitable for drought projections and changes under climate change (Vicente-Serrano, et al., 2020a). Similarly, for hydrological drought, Standardized Streamflow Index (SSI) only considers streamflow, whereas water managers may be interested in other hydrological components such as groundwater that may be critical in understanding the development and duration of drought events (Wossenyeleh et al., 2021).

Relatively few studies have employed multiple indices at the catchment scale to assess the link between meteorological and hydrological droughts and to understand the complex mechanisms of hydrometeorological drought propagation (Zhou et al., 2021). Zhou et al. (2021) introduced a nonlinear dependency indicator to examine propagation of meteorological to hydrological drought using a directed information transfer index. They concluded that drought propagation was primarily affected by the magnitude and frequency of meteorological drought events, together with the sensitivity of hydrological characteristics to drought. Similarly, H. K. Meresa et al. (2016) investigated the impact of climate change on hydrometeorological drought frequency and occurrence in Polish catchments, concluding that meteorological drought frequency was less than that of hydrological drought in lowland catchments. In contrast, in highland catchments, the frequency and magnitude of meteorological drought were greater than those of hydrological drought. Barker et al. (2016) used cross-correlation between the 1-month SSI and various SPI accumulation time scales to examine the relationship between meteorological and hydrological drought in the UK. Their results showed that at short aggregation time scales meteorological drought conditions have smaller spatial variability than longer accumulation periods. Shin et al. (2018) used Bayesian conditional probability theory to understand linkages and propagation between meteorological and hydrological drought using SPI and the palmer hydrological drought index (PHDI) finding that longer aggregation time scales result in higher probability of meteorological to hydrological drought propagation, and that the frequency of meteorological drought was greater than hydrological drought, whilst the severity of meteorological drought was often less than that of hydrological drought.

In Ireland, while a number of studies have investigated changes in precipitation and temperature (e.g., Nolan et al., 2017) and projected changes in seasonal and low flows (e.g., Golian & Murphy, 2021; H. K. Meresa et al., 2022; Romanowicz et al., 2016), little research has examined prospective changes in drought characteristics under climate change. To adapt to changes in hydrometeorological drought more knowledge regarding their likely changes, interlinkages, and propagation in the future is required. This study explores the impact of climate

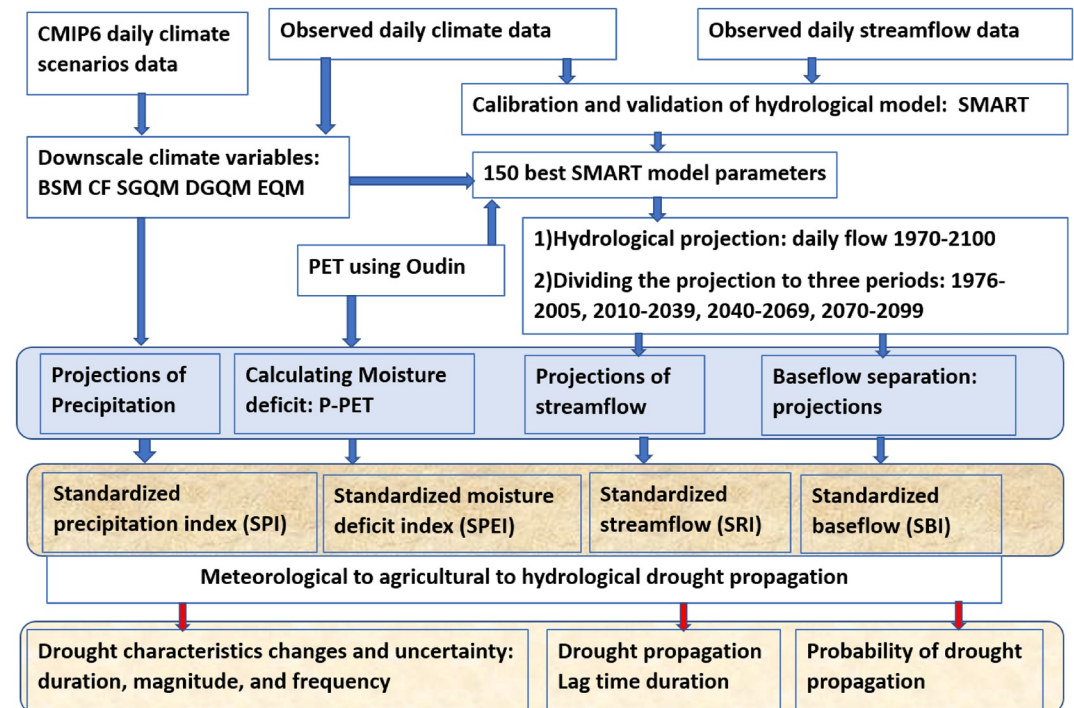


**Figure 1.** Steps involved in the study design in evaluating changing drought characteristics and propagation under changing climate.

change on hydrometeorological drought for 10 Irish catchments. Using indices representing different components of the hydrological system, changes in drought characteristics and propagation are examined. Specifically, we employ 12 Global Climate Models from the Coupled Model Inter-comparison Project phase 6 (CMIP6) (Eyring et al., 2016), forced with SSP370 and bias corrected to catchment conditions to force a conceptual hydrological model to generate hydrological projections for each catchment. We then fit standardized indices (SPI, SPEI, SSI, SBI) at different aggregation timescales (3, 6, and 12-months) to simulated variables to investigate changes in drought characteristics and their propagation at the catchment scale. The remainder of the paper is organized as follows. Data and methods are presented in Section 2. Section 3 provides the results, before Section 4 discusses the key findings and limitations of the study. Key conclusions are drawn in Section 5.

## 2. Data and Methods

Figure 1 provides an overview of the steps taken for examining future changes in drought characteristics and propagation for each study catchment. In the following sections details on the data and methods used are provided.

### 2.1. Study Catchments and Observed Data

Ten catchments were selected from across the island of Ireland with different hydroclimatic conditions, including catchment size, runoff coefficient (RC), climate elasticity, and groundwater storage (as measured by the Base Flow Index) (Table 1 and Figure 2). Each catchment has good quality discharge and meteorological data with limited urban land use and abstractions. Daily mean precipitation varies from 2.42 mm for the Dee to 5.41 mm for the Laune, while daily mean discharge ranges from 1.54 m<sup>3</sup>/s for Stradbally and 28.6 m<sup>3</sup>/s for the Laune catchment. The elasticity of runoff is inversely correlated to the RC. Daily precipitation, air temperature and discharge data were collected for the period 1976–2005 for each catchment. Discharge data were obtained from the Office of Public Works (OPW) and the Environmental Protection Agency (EPA). Meteorological data were extracted from gridded data sets (<https://www.met.ie/climate/available-data>) produced by Met Éireann (Irish Meteorological Agency) and averaged for each catchment. Estimates of PET were calculated using the Oudin method (Oudin et al., 2005), which shows relatively higher PET for eastern catchments.



**Table 1**  
List of Selected Catchments (See Figure 1 for Their Geographical Location)

Code	Flow station	Waterbody	Lat	Lon	Area (km <sup>2</sup> )	$P_{\text{mean}}$ (mm)	$Q_{\text{mean}}$ (m <sup>3</sup> /s)	BFI	RC	Ep	PETr
S06013	Charleville	Dee	53.856	-6.414	309	2.42	4.23	0.67	0.15	0.57	0.21
S12001	Scarawalsh	Slaney	52.549	-6.55	1,031	3.00	21.23	0.70	0.61	0.14	0.23
S14007	Derrybrock	Stradbally	53.039	-7.085	115	2.50	1.54	0.73	0.05	1.62	0.22
S15003	Dinin Bridge	Dinin	52.715	-7.292	140	2.81	5.91	0.53	0.18	0.48	0.22
S18050	Duarrigle	Blackwater	52.096	-9.097	250	4.36	7.59	0.48	0.15	0.57	0.24
S22035	Laune Bridge	Laune	52.062	-9.617	560	5.41	28.16	0.68	0.45	0.19	0.24
S23002	Listowel	Feale	52.443	-9.476	647	3.96	24.92	0.52	0.54	0.16	0.24
S25001	Annacotty	Mulkear	52.669	-8.529	648	3.25	15.36	0.64	0.41	0.21	0.23
S26029	Dowra	Shannon	54.192	-8.015	117	4.29	4.87	0.39	0.10	0.88	0.21
S33001	Glenamoy	Glenamoy	54.24	-9.696	76	4.45	2.88	0.43	0.06	1.55	0.22

Note. For each catchment, mean annual precipitation ( $P_{\text{mean}}$ ), mean annual streamflow ( $Q_{\text{mean}}$ ), streamflow elasticity to precipitation (Ep), runoff coefficient (RC), PET ratio of winter and summer (PETr), and baseflow index (BFI) are computed for the period 1976–2005.

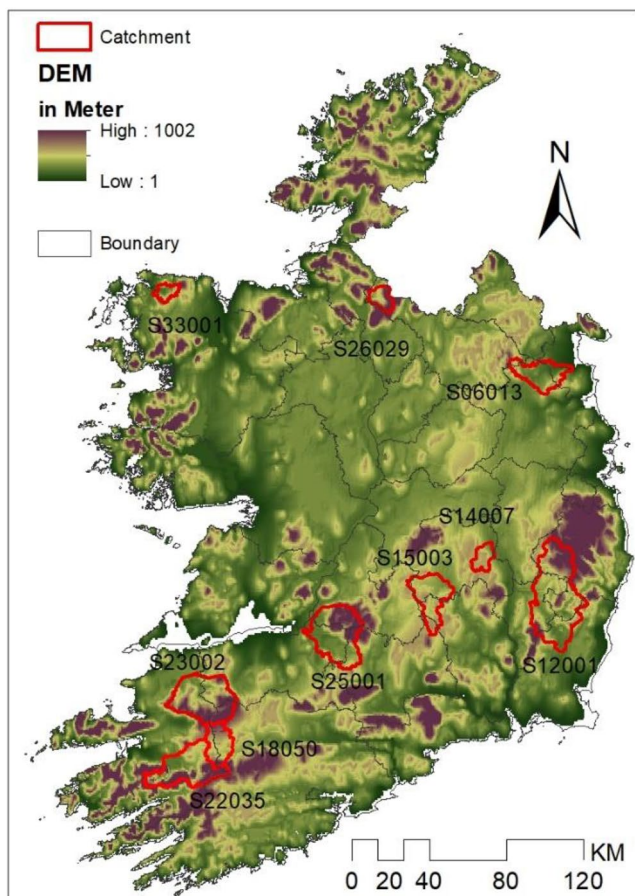


**Figure 2.** Location of the case study catchments. The catchment codes are represented as S06013 for Dee catchment, S12001 for Slaney, S14007 for Stradbally, S15003 for Dinin, S18050 for Blackwater, S22035 for Laune, S23002 for Feale, S26029 for Dowra, S25001 for Annacotty, and S33001 for Glenamoy.

## 2.2. Climate Models and Bias Correction

To evaluate the impact of climate change, daily air temperature and precipitation data from 12 earth system models (Table 2) comprising the Coupled Model Intercomparison Project Phase 6 (CMIP6) and forced using Shared Socioeconomic Pathway (SSP) SSP370 were extracted from the ESGF (Earth System Grid Federation) website (<https://esgf-node.llnl.gov/search/cmip6/>) for the period of 1976–2100. The grid cells closest to the catchment centroid were used to extract data for each catchment. Bias correction of each model was undertaken using the baseline period 1976–2005. Teutschbein and Seibert (2013) evaluated bias correction techniques for precipitation (including: linear scaling, local intensity scaling, power transformation, and distribution mapping (DM)) finding that DM offers promise for precipitation. Similarly, H. Meresa et al. (2021) examined five bias correction methods for flood projections in selected river catchments in Ireland, finding that quantile mapping is good at reproducing precipitation intensity on wet days. Here we employ three statistical bias correction techniques for precipitation: (a) the Change Factor (CF) technique as a simple and direct correction transfer from the historical to future period; (b) Empirical Quantile Mapping (EQM) based on pairwise comparison of the observed and simulated precipitation empirical cumulative density function (ecdf) during the reference period (1976–2005), and; (c) Distribution Quantile Mapping (DQM), whereby parameters are extracted by fitting a Gamma distribution to observed and simulated data and matching corresponding quantiles from observed and raw climate output during the period 1976–2005.

We applied two variants of DM: Single Gamma Quantile Mapping (SGQM) and Double Gamma Quantile Mapping (DGQM). These methods allow excess dry days, drizzle, and wet days to be considered and corrected. For SGQM, the Gamma distribution is fitted to the upper 75% of daily observed and simulated precipitation. For DGQM, the Gamma distribution is fitted to the upper 25% and lower 25% of observed and simulated precipitation. A detailed description of these methods is presented in H. Meresa et al. (2021). For temperature, we employ EQM only. Bias correction techniques were assessed using Pearson's correlation (RR), relative Bias and the Murphy skill score (SSM) (A. Murphy, 1988) which measures repro-

**Table 2**  
List of Coupled Model Inter-Comparison Project Phase 6 Climate Models Employed in This Study

Code	Institute	Parent source Id	Institution Id
CM1	Scientific and Industrial Research Organization, Australia	ACCESS-CM2	CSIRO
CM2	Beijing Climate Center, China	BCC-CSM2-MR	BCC
CM3	National Center for Atmospheric Research, USA	CESM2	NCAR
CM4	European: EC-EARTH consortium	EC-Earth	EC-EARTH consortium
CM5	Global Fluid Dynamics Laboratory, USA	GFDL	NOAA-GFDL
CM6	Met Office Hadley Center, UK	HadGEM3-GC31-LL	MOHC
CM7	JAMSTEC, AORI, NIES, and R-CCS, Japan	MIROC6	MIROC
CM8	Max Planck Institute for Meteorology, Germany	MPI-ESM1-2-HR	MPI-M
CM9	Meteorological Research Institute, Japan	MRI-ESM2-0	MRI
CM10	Nanjing University of Information Science and Technology, China	NESM3	NUIST
CM11	NorESM Climate modeling Consortium, Norway	NorESM2-LM	NCC
CM12	Met Office Hadley Center, UK	UKESM1-0-LL	MOHC

duction of observed drought characteristics in the reference period (1976–2005) at different SPI time scales. Having bias corrected climate model outputs for each catchment, projected changes were evaluated for the 2020s (2010–2039), the 2050s (2040–2069) and the 2080s (2070–2099) with respect to the reference period (1976–2005).

### 2.3. Hydrological Model

The Soil Moisture Accounting and Routing for Transport (SMART) hydrological model (Hallouin et al., 2020; Mockler et al., 2016) was used to simulate river flow. The model takes precipitation and potential evapotranspiration as inputs and consists of 10 parameters that govern five catchment flow pathways, each represented as a single linear storage (including overland flow, interflow, drain flow, shallow, and deep groundwater flow). As described by Hallouin et al. (2020), soil moisture storage is estimated by whether conditions are water-limited ( $PET > P$ ) or energy-limited ( $PET < P$ ). Effective precipitation during energy-limited conditions is obtained by applying a scaling correction parameter ( $\theta T$ ) and subtracting any direct soil evaporation. The parameter  $\theta H$  determines any direct surface runoff. Surplus precipitation infiltrates into the soil, represented by six layers with a total moisture capacity of  $\theta Z$ . Once the moisture-holding capacity of a layer is exceeded, surplus moisture percolates downwards to a deeper layer if it has capacity, otherwise it is intercepted by drains or eventually moves to shallow or deep groundwater stores. When  $PET < P$ , the model meets demands by evaporation from the soil layers, starting at the first layer and incrementally moving to the lower layers. The parameter  $\theta C$  represents evaporation decay as layers dry up. The outputs of each flow path are routed through a single linear reservoir, representing river routing ( $\theta RK$ ).

Calibration and validation were carried out using observations for 1990–2007 and 2008–2015, respectively. Using Latin Hypercube Sampling (C. Murphy et al., 2006), 30,000 parameter sets were sampled from a uniform distribution representing each model parameter. The resultant parameter sets were then evaluated against observations for the validation period in each catchment using the logarithmic Nash Sutcliffe Efficiency (LogNSE) objective function (Nash & Sutcliffe, 1970) given our focus on drought. LogNSE is defined as;

$$\text{LogNSE} = 1 - \frac{\sum_{t=1}^j (\ln(Q_{o,t}) - \ln(Q_{m,t}))^2}{\sum_{t=1}^j (\ln(Q_{o,t}) - \ln(\bar{Q}_o))^2} \quad (1)$$

where  $Q_{o,t}$  and  $Q_{m,t}$  are observed and simulated flow at time  $t$ ,  $Q_o$  is the mean observed flow and  $j$  is the length of the  $j$ th time series. The best 150 parameter sets were retained to derive future simulations, with results focused on the median simulation from 150 parameter sets.

#### 2.4. Baseflow Separation

Baseflow is the sum of delayed shallow and deep subsurface flow that sustains river flow between periods of excess precipitation and represents the groundwater recession component of streamflow. Understanding how baseflow is affected by climate change is critical for water resources management and in-stream ecohydrological health. Separation of streamflow into surface runoff and baseflow is commonly implemented using automatic baseflow digital filter (BFlow) techniques by passing the filtering equation three times through the daily streamflow time series (Bosch et al., 2017). Here we use a commonly applied recursive filtering technique to identify baseflow:

$$BF_t = \alpha * BF_{t-1} + \frac{1-\alpha}{2} * (Q_t + Q_{t-1}) \quad (2)$$

where BF is the baseflow at time  $t$ ,  $\alpha$  is the filter parameter,  $Q_t$  is the total streamflow at time  $t$ . This method is applied under only one condition,  $BF \leq Q_t$  (Eckhardt, 2008). We calibrate and validate this method using observed groundwater stage time series data to get stable filter parameters (Eckhardt, 2008).

#### 2.5. Drought Indices

We employ four hydrometeorological drought indices, namely; the SPI (Mckee et al., 1993), the Standardized Precipitation-Evapotranspiration Index (SPEI) (Vicente-Serrano, et al., 2020a), the SRI (Shukla & Wood, 2008) and the Standardized Baseflow Index (SBI). The parameters of each index are calculated in the reference period (1976–2005) and utilized to project hydro-meteorological drought into the future. We characterized each drought index at three different accumulation timescales (3, 6, and 12-months) using running sums of precipitation and moisture deficits (for SPI and SPEI, respectively) and averages of runoff and baseflow (for SSI and SBI, respectively). The following paragraphs summarize derivation of each index.

The mathematical formulation of SPI depends on the distribution of precipitation. In this study, if the monthly accumulated precipitation distribution is normal, then SPI is calculated based on simple Z-score statistics. Otherwise, we used a two-parameter gamma distribution to calculate the drought index.

$$Z_{score} = \frac{X - \bar{X}}{\sigma} \text{ or } f(X; \alpha, \beta) = \frac{1}{\beta^\alpha \int_0^\infty X^{\alpha-1} e^{-X/\beta} dx} X^{\alpha-1} e^{-X/\beta}, \text{ for } x > 0 \quad (3)$$

where the Z-score standardized value,  $X$  is aggregated monthly precipitation, and  $a$  and  $b$  are the scale and shape parameters of the Gamma distribution, estimated using the maximum likelihood estimation (MLE) method.

SPEI is derived using aggregated monthly precipitation (Pre) and potential evapotranspiration (Pet). The moisture deficit (Mosdef) is calculated through simple subtraction,

$$\text{Mosdef} = \text{Pre} - \text{Pet} \quad (4)$$

and fitted to a three parametric log-logistic distribution following Vicente-Serrano et al. (2010), and given as:

$$f(\text{Mosdef}; \beta, \gamma) = \frac{\left(1 + \frac{\gamma(\text{Mosdef}-\alpha)}{\beta}\right)^{-(1/\gamma+1)}}{\beta \left[1 + \left(1 + \frac{\gamma(\text{Mosdef}-\alpha)}{\beta}\right)^{1/\gamma}\right]^2} \quad (5)$$

where  $\beta$ ,  $\alpha$ ,  $\gamma$  are the scale, location, and shape parameters, respectively, estimated using MLE. The estimated log-logistic probabilities were then transformed into a standard normal distribution.

For SSI, we used average monthly flow fitted to a lognormal distribution:

$$f(X; \mu, \sigma) = \frac{1}{X} * \frac{1}{\sigma\sqrt{2\pi}} \exp\left(-\frac{(\ln - \mu)^2}{2\sigma^2}\right), \text{ for } X > 0 \quad (6)$$

where  $x$  is the streamflow, and  $\sigma$  and  $u$  are the scale and location parameters of the lognormal distribution estimated by MLE. The estimated probabilities were transformed into a standard normal distribution.

Finally, for SBI, we used average monthly baseflow fitted to a normal distribution, and then calculated based on simple Z-score statistics:

$$Z_{\text{score}} = \frac{X - \bar{X}}{\sigma} \quad (7)$$

where the Z-score standardized value,  $X$  is average monthly baseflow.

We analyze standardized indices in two ways. First, we examine changes in the magnitude of annual and seasonal mean standardized series for each future period relative to the reference period. For SPI, SPEI, SSI, and SBI winter [DJF] is represented by February 3 month accumulations (e.g., February SPI-3), spring [MAM] by May, summer [JJA] by August and autumn [SON] by November. To evaluate annual deficits, we utilize a 12-month accumulation for December, while summer and winter half years are represented by 6-month accumulations in September and March, respectively. We also examine changes in the frequency of seasonal and annual drought by counting the number of seasons/years in each 30-year period in which accumulated totals fall below the threshold of  $-0.5$ . Second, we also examine changes in the characteristics of drought events identified for each metric using a 3-month accumulation period. Again, a threshold of  $-0.5$  was selected to indicate the onset of drought conditions, as it is commonly used in Ireland (Falzoi et al., 2019; C. Murphy et al., 2018; Noone et al., 2017). Both the average duration and frequency of drought events was evaluated for each future period, relative to the reference period.

## 2.6. Drought Propagation

Drought propagation refers to the transfer of meteorological deficits to other components of the hydrological system (i.e., soil moisture deficits, streamflow deficits and/or groundwater deficits) (Eltahir & Yeh, 1999). The time taken for propagation is important for water managers (Apurv et al., 2017; Barker et al., 2016). To examine propagation, we derive the conditional probability of two dependent drought conditions (Pontes Filho et al., 2019; Ribeiro et al., 2019), that is, the probability of SPI drought propagating to SSI and SBI. For two drought indices with their respective lag time  $t_g$ , we used the posterior and prior pairs of probabilities of SPI with SRI or SBI, and links were developed to indicate the direct influence of one on the another. Using the example of SPI and SSI this can be expressed as:

$$P(\text{SSI}_i | \text{SPI}_j \in t_{g_m}) = \frac{P(\text{SSI}_{i,m}, \text{SPI}_{j,m})}{P(\text{SPI}_j)} \quad (8)$$

where,  $P(\text{SSI}|\text{SPI})$  is the conditional propagation probability to SSI drought given SPI,  $P(\text{SPI}, \text{SSI})$  is the sum of individual and combined probabilities at a specific lag time,  $t_{g_m}$  is the optimal lag time, identified as the strongest correlation between respective drought conditions. The subscripts  $i, j$ , and  $m$  represent the meteorological drought series ( $i$ ), hydrological drought series ( $j$ ) at specific drought timescale ( $m$ ).

Lag times and the probability of drought propagation from one type to another (using Equation 8) were estimated for each catchment using SPI, SSI, and SBI at 3 and 12-month accumulation timescales for both historical and projected future periods using the ensemble mean of projected changes. As there are different lagged responses for each drought event, the average drought propagation lag time was calculated.

## 3. Results

### 3.1. Hydrological Model Calibration/Validation and Bias Correction

Overall, LogNSE, PBIAS in baseflow index (the ratio of runoff to total streamflow), and the ratio of observed streamflow-precipitation elasticity (QPobs) to simulated streamflow-precipitation elasticity (QPest) were used to assess model performance. Table 3 shows calibration and validation results for the LogNSE objective function for each catchment. Calibration scores range from 0.83 (Slaney) to 0.91 (Annacotty), while validation scores range from 0.66 (Dowra) to 0.95 (Laune), indicating good fit to the observed time series. PBIAS values in BFI range from 0.66 (Dowra) to 13.52 (Annacotty), while validation scores range from 1.19 (Blackwater) to 22.48 (Glenamoy), indicating low PBIAS error in fitting to observed BFI time series. The Glenamoy station had the highest PBIAS (22.48%), which is not directly reflected in a higher BFI but rather in a lower BFI and a higher

**Table 3**

*Soil Moisture Accounting and Routing for Transport Model Performance Using Logarithmic NSE (LogNSE) Objective Function, Percent of Bias (PBIAS) in Baseflow (BFI) Values, and Streamflow-Precipitation Elasticity Values (Relative Difference in %) in the Calibration (Cal) From 1990 to 2007 and Validation (Val) From 2008 to 2015 Period*

Catchment code	Flow station	Waterbody	LogNSE		PBIAS: BFI		QPobs/QPsim	
			Cal	Val	Cal	Val	Cal	Val
S06013	Charleville	Dee	0.9	0.9	-1.48	5.83	17.51	16.53
S12001	Scarrawalsh	Slaney	0.83	0.84	-0.38	8.46	28.26	24.64
S14007	Derrybrock	Stradbally	0.86	0.9	-2.28	3.33	34.19	35.21
S15003	Dinin Bridge	Dinin	0.87	0.86	3.06	11.11	40.66	43.06
S18050	Duarrigle	Blackwater	0.91	0.88	0.90	1.19	17.46	18.01
S22035	Laune Bridge	Laune	0.93	0.95	1.87	-1.70	13.36	11.34
S23002	Listowel	Feale	0.91	0.90	8.94	12.88	12.84	14.48
S25001	Annacotty	Mulkear	0.91	0.87	13.52	15.17	16.18	14.16
S26029	Dowra	Shannon	0.85	0.66	2.46	1.49	13.59	18.82
S33001	Glenamoy	Glenamoy	0.84	0.84	12.37	22.48	12.33	17.65

PBIAS value. Furthermore, the sensitivity of changes in streamflow to changes in precipitation was also used to compare between the observed and simulated time series. The ratio of QPobs to QPsim values range from 12.33 (Glenamoy) to 40.66 (Dinin) in the calibration period, and from 11.34 (Laune) to 43.06 (Dinin) in the validation period.

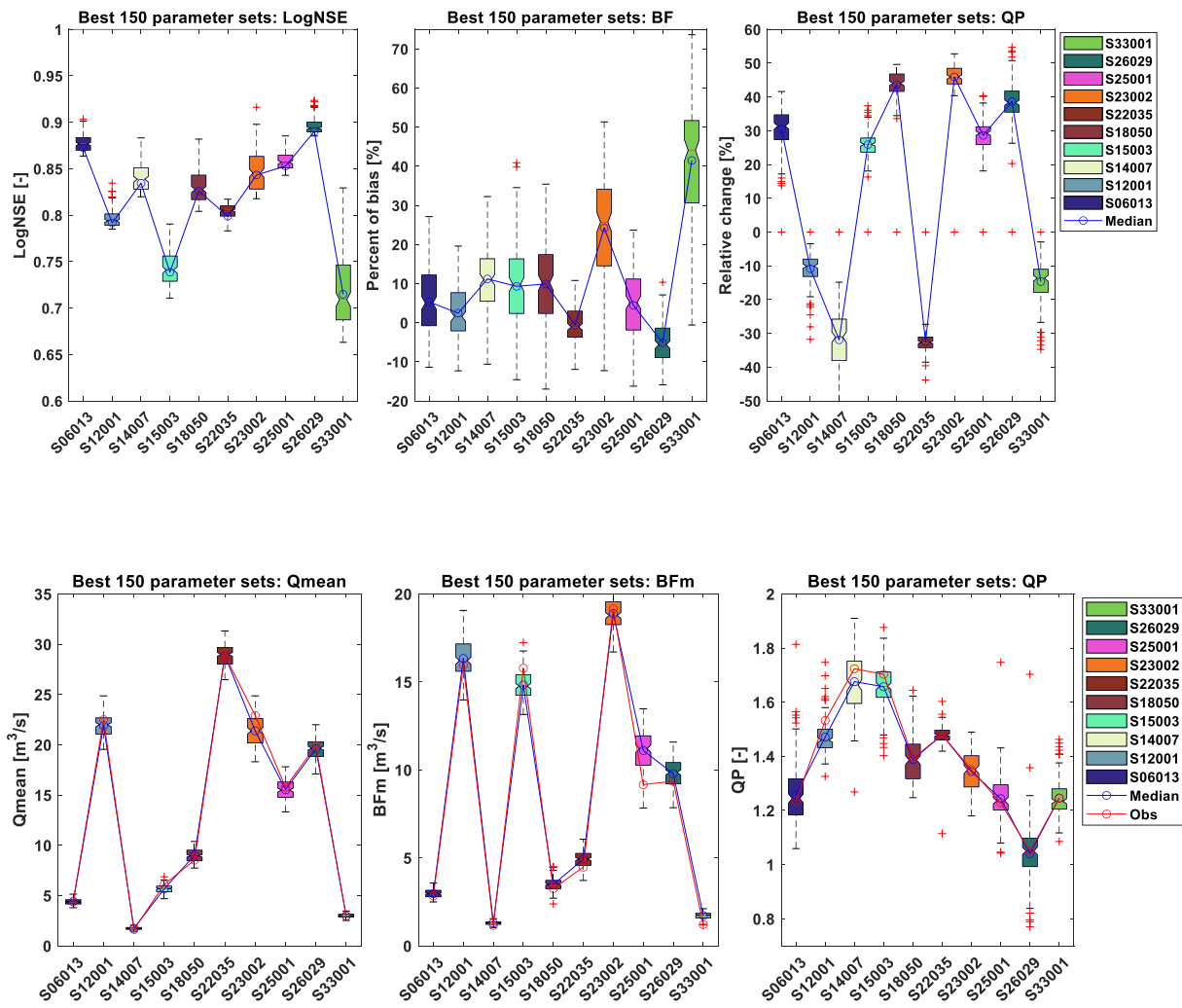
Similarly, the spread of the 150 best simulations were evaluated using LogNSE, PBIAS of BFI, and the ratio of elasticity of streamflow to precipitation in the calibration period (Figures 3a and 3b). Overall, the spreads (box sizes) of LogNSE, PBIAS (of BFI), and the relative change of the elasticity (QP) are small across the catchments. However, these values showed a clear spatial difference among the catchments. For instance, Dowra shows the highest values of LogNSE, Laune the smallest PBIAS, and Slaney the smallest relative change in elasticity. The Glenamoy catchment, on the other hand, has lower LogNSE values, the highest PBIAS, and the highest QP. Therefore, the performance is acceptable across all the catchments in reproducing the observed  $Q_{\text{mean}}$ , BF, and QP.

Figure 3b depicts the performance of the 150 best simulation indices by comparing the median of these simulations to observed time series of  $Q_{\text{mean}}$ ,  $BF_{\text{mean}}$ , and QP. These results are more consistent with the static performance in Figure 3a. The simulation spread is small across the selected catchments, indicating that the uncertainty in hydrological parameters is small.

Bias correction results are presented in Figure 4. Methods perform differently across catchments and drought time scales, but all methods outperform use of the raw climate model projections. SSM values  $<0$  indicate higher bias and lower spread of residual errors between observed and simulated drought magnitude. For seasonal drought magnitude, the SSM is near to zero for all bias correction methods, indicating that the simulation error/bias is smaller and has higher accuracy in reproducing the historical drought magnitude. Correlation scores range from 0.2 to 0.6, while the relative bias ranges from 0.3 to 1.3, and SSM ranges from 0 to  $-2.0$  across the catchments and bias correction methods. Raw GCM outputs show the highest relative bias and lowest correlation scores.

DGQM shows a higher correlation with observed drought magnitude at the 3-month accumulation period, whereas EQM performed best at the 6- and 12-month accumulation time scale. However, performance is not the same across catchments and time scales. 3-month SPI indices have lower bias than 6- and 12-months SPI indices for different bias correction techniques. In addition, the SSM scores differ considerably across catchments for SPI3 and SPI12, while they are less varied for summer and autumn drought magnitude detection. Interestingly, the bias correction approach tends to have greatest influence on drought magnitude, and overall, the DGQM shows better performance in reproducing seasonal drought magnitudes across the catchments. CF and BSM show a weaker correlation and higher bias with observed meteorological drought magnitude using SPI. In general, the Dowra, Dinin, and Laune catchments show weak correlation, high bias and lower SSM across aggregated time scales. Overall, the DGQM bias correction method performed best in reproducing drought magnitude across the catchments, therefore we employ this method for further analysis.





**Figure 3.** (a). Performance scores for all 150 parameter sets in reproducing the observed streamflow: (a) logNSE, (b) BF, and (c) QP. Each boxplot represents the 150 simulations for each catchment. The blue line represents the median of the 150 simulations. (b) The performance of 150 hydrological parameter sets in reproducing the observed streamflow: (a) logNSE, (b) BF and (c) QP. Boxplots represents simulations from the best 150 parameter sets. The blue line represents the median of the 150 simulations, and the red circle represents the observed values.

### 3.2. Projected Changes in Precipitation, Moisture Deficient, Streamflow, and Baseflow

We examine changes in seasonal precipitation, moisture deficits (P-E), discharge and baseflow simulations for the 21st century from our ensemble of 12 bias corrected climate models under SSP370. Figure 5 shows relative change in monthly precipitation, mean moisture deficit, mean flow, and mean baseflow for each catchment for the 2020s, 2050s, and 2080s. Large decreases in summer precipitation and increases in winter and spring are evident. Summer decreases show a wide range for each variable, becoming larger as the century progresses. For summer precipitation, a mean reduction of ~6% across catchments is evident for the 2020s, ~17% by the 2050s, and ~40% by the 2080s. Likewise, moisture deficits are projected to become larger in summer due to higher evaporative losses with increasing temperature. The largest decreases are noted for baseflow in summer season, with mean reductions across catchments ranging from ~10% in the 2020s to ~50% in the 2080s. Overall, there is a substantial summer reduction in mean flow and groundwater in the low water period in catchments Stradbally, Dinin, and Feale. The summer hydroclimatic changes at Dee, Slaney, and Laune are relatively smaller.

### 3.3. Changes in Seasonal and Annual Standardized Drought Indices

Figures 6a and 6b show the relative changes in seasonal and annual standardized indices and the frequency of seasonal/annual droughts for each catchment for the 2050s and 2080s under SSP370. The boxplots show a

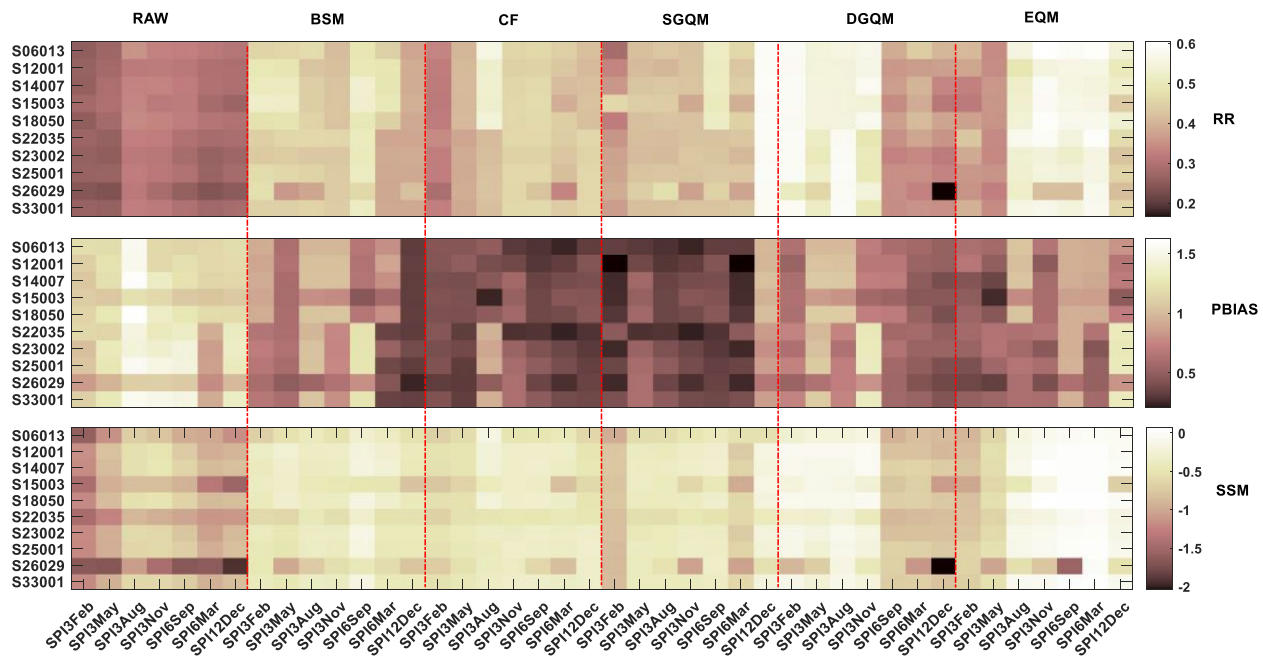


**Figure 4.** Correlation (RR), relative bias (Bias) and skill score deviation (SSM) of drought magnitude for each catchment from climate models bias corrected using each of the five methods, together with raw climate model projections, relative to observed data in the reference period (1976–2005). Standardized Precipitation Index is derived at 3, 6, and 12-month time scales.

wide range of changes in both magnitude and frequency, with a tendency for decreased drought magnitude in all seasons except summer in most catchments. In summer, drought magnitude and frequency are increased by 50% and 20%, respectively, in the 2050s and by a further 10% by the 2080s for meteorological drought (SPI). Similarly, hydrological indices (SSI and SBI) show increasing summer drought magnitude and frequency in the

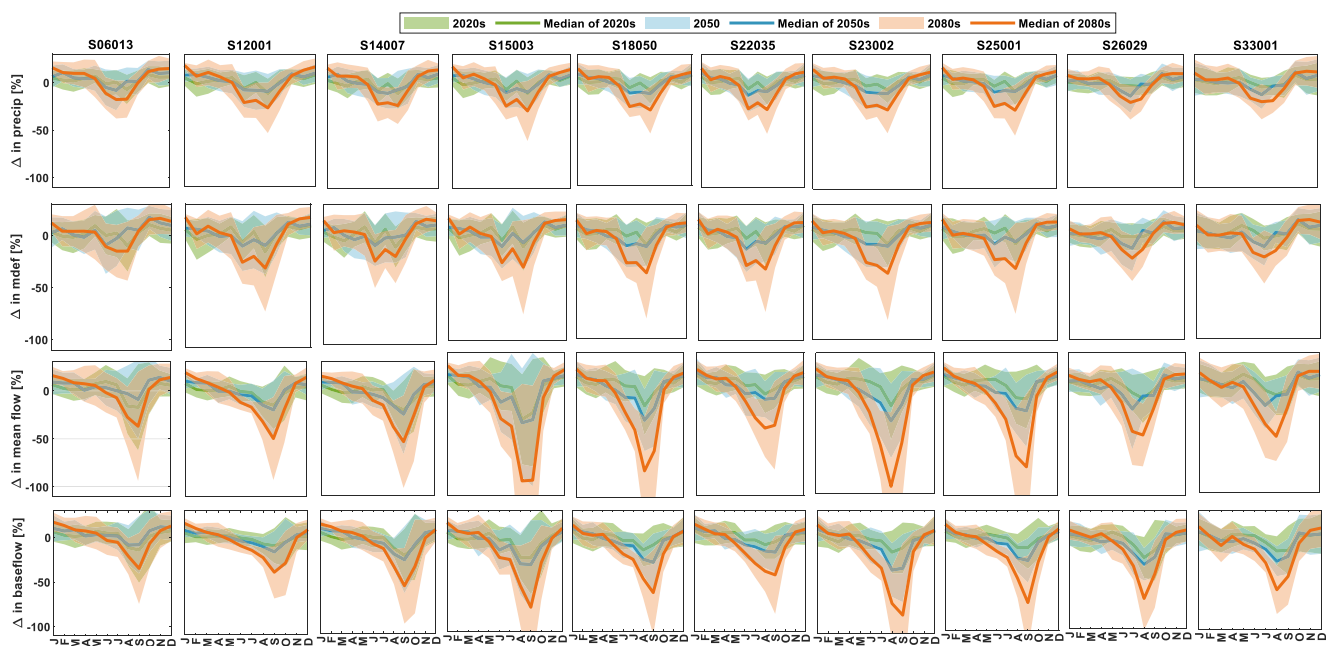


**Figure 5.** Changes (%) in seasonal precipitation (first row), mean moisture deficit (second row), mean flow (third row), and mean baseflow (last row) in the 2020s (green shaded and green solid line), the 2050s (blue shaded and blue solid line), and 2080s (orange shaded and orange solid line) for each catchment with respect to the reference period (1976–2005) under SSP370. Shaded area and line show the spread and ensemble median from 12 Coupled Model Inter-comparison Project phase 6 climate models bias corrected using Double Gamma Quantile Mapping.



**Figure 6.** (a) Change (%) in seasonal and annual hydrometeorological drought magnitude in the 2050s (left: 2040–2069) and 2080s (right: 2070–2099) for each catchment using Standardized Precipitation Index, Standardized Precipitation Evapotranspiration Index, Standardized Streamflow Index, and Standardized Baseflow Index under SSP370. Boxplots show the spread of 12 climate models bias corrected using Double Gamma Quantile Mapping. Boxplots show the median and interquartile range (IQR) of simulated changes with black dots indicating changes outside the IQR. (b) As per Figure 5 but for changes (%) in seasonal and annual drought frequency.

2050s and 2080s. However, SPI and SPEI show a lower spread and variability than SSI and SBI in the 2050s and 2080s, indicating that meteorological drought is less variable and uncertain than hydrological drought. Changes in autumn drought are small compared to the summer in most catchments and periods.



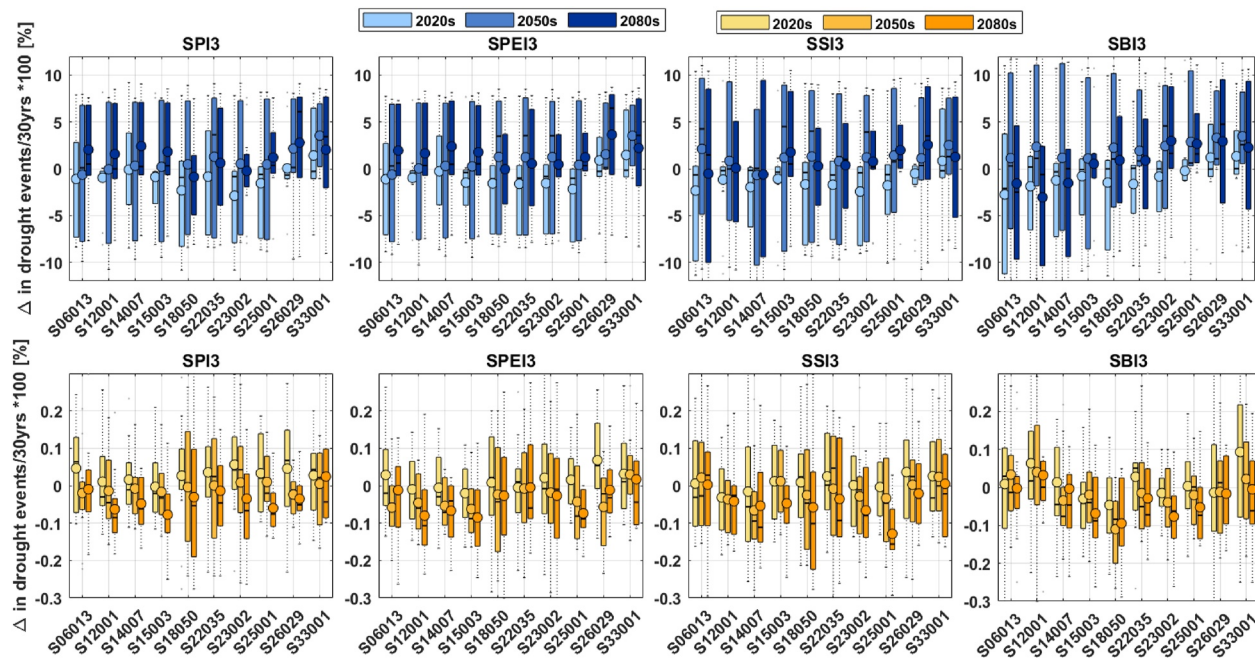


**Figure 7.** Changes in the average duration (months) and frequency of drought events in each catchment and future period for Standardized Precipitation Index, Standardized Precipitation Evapotranspiration Index, Standardized Streamflow Index, and Standardized Baseflow Index. Boxplots show the spread of 12 climate models bias corrected using Double Gamma Quantile Mapping. Boxplots show the median and interquartile range (IQR) of simulated changes with black dots indicating changes outside the IQR.

Annual (December SPI-12), spring (March SPI-3) and summer half year (September SPI-6) droughts show decreasing magnitude and frequency across catchments and indices (Figure 5). Modest differences in drought changes among the catchments are evident. In the 2050s, catchments Annacotty, Dowra, and Glenamoy shows relatively smaller change in magnitude and frequency during summer and spring. In the 2080s, changes typically become progressively greater across catchments. However, for Stradbally and Dee a decrease in drought frequency and magnitude from 2050s to 2080s is evident. Overall, the mean drought frequency and magnitude changes are much higher in the future in most catchments and range from  $-20\%$  to  $+50\%$  for SPI and SPEI and  $-30\%$  to  $70\%$  for SSI and SBI.

### 3.4. Changes in Drought Event Duration and Frequency

Figure 7 shows projected changes in average drought duration and event frequency in each catchment derived from indices with 3-month accumulation. Modest changes in event duration and frequency are simulated for the 2080s, despite the large reductions in precipitation and increases in magnitude simulated for summer above. This is due to the increased mean and variability of precipitation in winter and spring in most catchments. The direction of change in drought duration is uncertain for all indices for the 2020s and 2050s. However, by the 2080s drought duration for SPI-3 and SPEI-3 events is projected to increase, by up to 8 months in some catchments. For SSI-3 the direction of change remains uncertain for all future time periods, while for SBI-3 drought duration is projected to increase in catchments with least groundwater storage (low BFI, see Table 1).

The direction of change in the frequency of droughts is uncertain for most catchments in the 2020s and 2050s (Figure 7). For the 2080s some catchments show a clear signal toward decreased drought event frequency across different indices. For SPI-3 events Slaney, Stradbally, Dinin, Annacotty and Dowra show decreases in frequency, typically within the  $-10\%$  range. Decreased frequencies are also returned for SPEI-3 by the 2080s for catchments Slaney, Stradbally, Dinin, and Annacotty. For SSI-3 only catchments Dinin and Annacotty show a clear signal of decreased drought frequency by the 2080s, while catchments Feale and Annacotty show decreases in the frequency of SBI-3 events. Again, this is despite large reductions in summer precipitation and increased drought magnitude simulated for summer above.



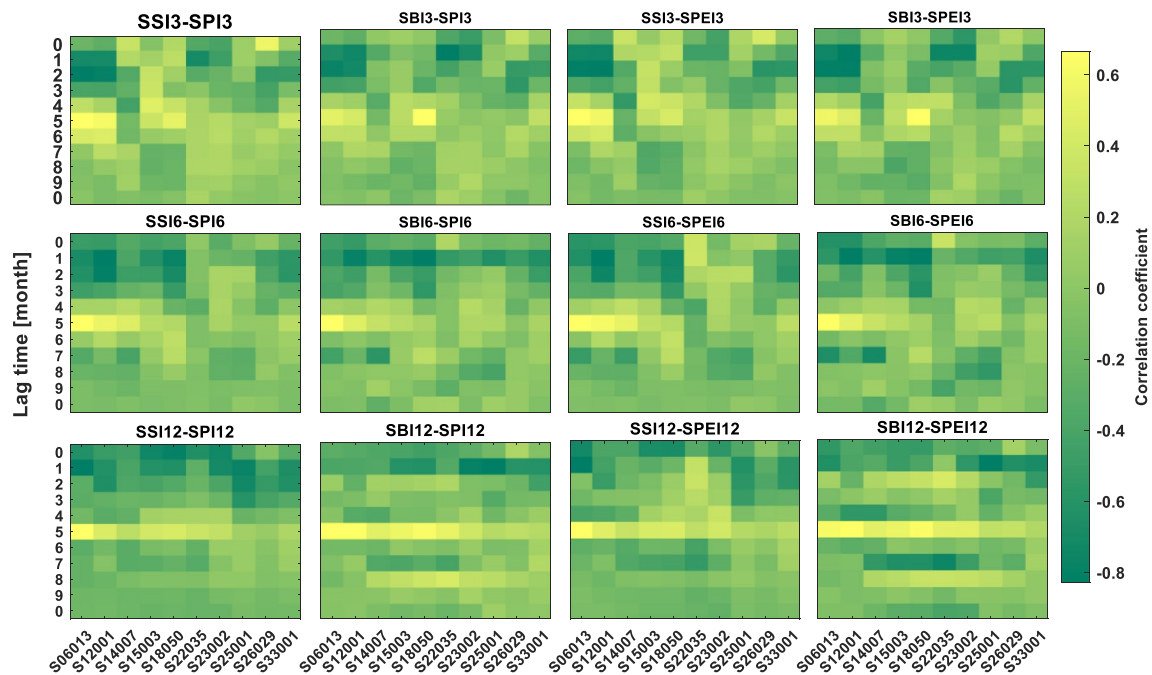


**Figure 8.** Lagged correlation between meteorological (Standardized Precipitation Index and Standardized Precipitation Evapotranspiration Index) and hydrological drought (Standardized Streamflow Index and Standardized Baseflow Index) indices for 3, 6, and 12-month accumulation periods during the reference period (1976–2005).

### 3.5. Lag Time Between Meteorological and Hydrological Droughts

The lag times and respective correlation coefficients for drought occurrence at different accumulation periods using SPI, SPEI, SSI, and SBI indices are shown in Figures 8–10 for the reference and future periods. Most catchments show similar lags between meteorological and hydrological drought occurrence at specific accumulation periods. As the accumulation timescale increases, the lag times of drought occurrence also increase. On average, the lag time for the three-month accumulation period is 3-months, whereas for the 12-month accumulation period it increases to almost 5-months. This is mainly related to the catchments' response to seasonal precipitation and catchment storage. For Dee and Slaney have unstable correlation across different lag times. This may be due to the drainage area and shape of the catchments affecting the lag time.

SSI and SBI have a reasonable correlation ranging from 0.2 to 0.4 across a wide range of lag times at the 12-month accumulation period, while SPI and SPEI have a good correlation ranging from 0.4 to 0.6, especially at a 4-month lag time. This implies that the connection between the surface and groundwater is crucial and plays a major role in controlling streamflow and groundwater drought in most catchments. For the 2050s and 2080s correlation between meteorological and hydrological drought increase for longer lags, with strongest correlations after 4–6 and 5–7 months in the near and far future, respectively (Figures 9 and 10). This indicates that the lag times between the meteorological drought and hydrological drought is likely to increase with climate change, with the time taken for precipitation anomalies to become apparent in hydrological variables increasing. This likely results from increases in precipitation in winter and spring, with associated increased in water storage which maintains baseflow contributions during meteorological drought onset. These were tested using the *t*-test statistical method, which confirmed that both meteorological drought and hydrological drought do not have the same mean and standard deviation (Table S1 in Supporting Information S1). Almost all the catchment showed a consistent result with the propagation probability that the one-to-one relationship between the meteorological drought and hydrological is not significant (Table S1 in Supporting Information S1).

### 3.6. Changes in Drought Propagation Probability

The probability of meteorological drought propagating to hydrological drought conditions (SSI and SBI) was estimated using conditional likelihoods at a given lag time for both 3- and 12-month accumulation periods using the ensemble mean (Figure 11). The time lag between the hydrological and meteorological drought was found to average

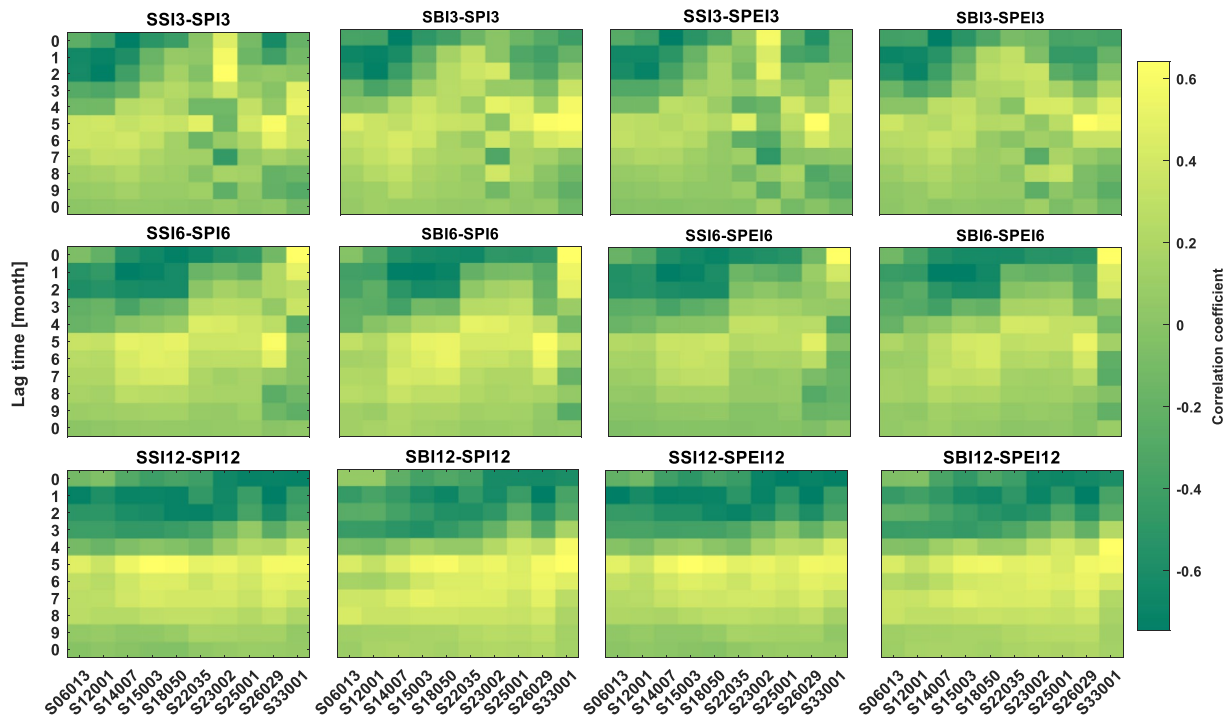


Figure 9. As per Figure 8 but for the 2050s (2040–2069).

3–5 months during the reference period and 5–7 months in the 2080s. The conditional probability of meteorological drought propagation from SPI to SBI (0.36) is higher than to SSI (0.3) at a 3-month accumulation timescale in the reference period. For future periods (2020s, 2050s, 2080s), the probability of drought propagation increased slightly. Largest increases are found for the 2050s in catchment Dee which shows a 7% increase in the probability of SPI-3 drought propagating to SSI drought. Changes in probability of <5% are found for other catchments. Similar results

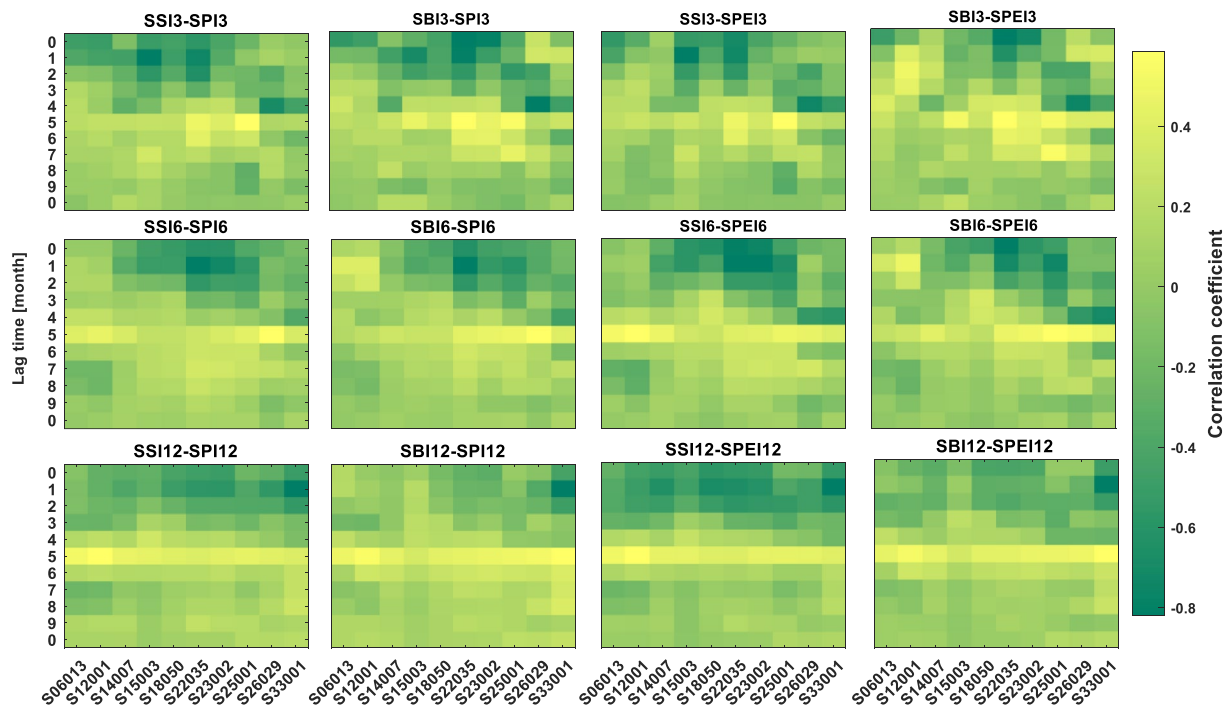


Figure 10. As per Figure 8 but for the 2080s (2070–2099).



**Figure 11.** The probability of meteorological to hydrological drought propagation in each catchment between standardized series at 3 and 12-month accumulation periods. Results are provided for the reference and future time periods from the ensemble mean of 12 Coupled Model Inter-comparison Project phase 6 models forced with SSP370 and bias corrected using Double Gamma Quantile Mapping.

are found for propagation of SPI to SBI drought at 3-month accumulation for the future time periods with catchment S06013 showing largest changes. Overall changes in drought propagation for 3-month accumulations are modest.

For the 12-months accumulation period the probability of drought propagation from SPI to SSI ranges from 0.39 (Dee) to 0.53 (Glenamoy) during the reference period. For SPI to SSI catchments Blackwater and Feale show a 7 and 6% increase in probability of drought propagation for the 2020s, respectively. For the 2050s catchment Dee shows an increase of 11%, increasing to 13% by the 2080s. Other catchments tend to show increases in SPI to SSI propagation probability, but typically less than 10% during the 2050s and 2080s. Largest increases are found for SPI to SBI propagation probabilities. During the reference period propagation of meteorological to groundwater drought is smallest for Dee (0.35) and largest for Stradbally and Dinin (0.40). For the 2020s catchments showing more than 10% increase in propagation probability include Dee (14%) and Stradbally (10%). By the 2050s all catchments show an increase in probability, greatest for Dee (19%), Stradbally (15%) and Slaney (11%). Increases in the probability of drought propagation from SPI to SBI are not as high for the 2080s, indicating the importance of increases in winter and spring precipitation in offsetting drought propagation to baseflow.

#### 4. Discussion

This study evaluated changes in drought characteristics and propagation with climate change for 10 Irish catchments. Bias corrected output from 12 GCMs comprising the CMIP6 ensemble and forced using SSP370 were used to run the SMART hydrological model for future time periods. A baseflow separation routine was used to disaggregate baseflow as an indicator of groundwater storage. Standardized drought indices (SPI, SPEI, SSI, and SBI) were then used to examine changes in seasonal and annual drought, the duration and frequency of drought events and the propagation to meteorological to hydrological drought events for future time periods, relative to the reference period (1976–2005).

Our results indicate substantial changes in monthly/seasonal precipitation that drive changes in droughts. While ranges of change are large and span a sign change, summer [JJA] precipitation shows large reductions (ensemble mean reduction across catchments of  $-40\%$  by the 2080s), becoming increasingly large as the century progresses. Concurrent increases in evaporative demand result in increases in summer soil moisture deficits (P-PET) of greater magnitude than reductions in precipitation alone. In summer, large decreases in discharge and baseflow are also simulated, with the latter showing a mean decrease of  $-50\%$  across catchments by the 2080s. Outside of summer, winter [DJF] precipitation shows a tendency for increases, becoming progressively larger as the century progresses, while the direction of change in spring [MAM] and autumn [SON] precipitation is uncertain. Similar changes are evident for discharge and baseflow. Changes in precipitation and discharge are very much in line with previous research in Irish catchments (H. K. Meresa et al., 2022; C. Murphy et al., 2023). Therefore, the key season for changes in drought is summer, with changes in precipitation in winter and spring important in setting antecedent conditions in relation to catchment wetness and groundwater storage.

For seasonal droughts, while a wide range of change is apparent there is a tendency for decreases in the magnitude and frequency of droughts on an annual basis and in all seasons except summer. Summer (August 3-month accumulation) shows large increases in the magnitude and frequency of drought in all components of the hydrological system (SPI, SPEI, SSI, SBI) by mid-century. Hänsel et al. (2019) showed similar seasonal drought characteristics, with dryness becoming more pronounced for summer and a wetting trend in autumn and winter in central Europe. Spinoni et al. (2018) also highlight that drought frequency and magnitude are projected to increase in summer and spring over southern Europe, and less intensely in winter and autumn. Notably, summer SSI and SBI show larger variability than SPI and SPEI indicating the non-linear translation of meteorological to hydrological drought and the additional uncertainty associated with hydrological modeling (H. K. Meresa & Zhang, 2021; Mockler et al., 2016). Such increases in the magnitude and frequency of summer droughts would have substantial management implications for Irish water resources and agriculture where the recent summer drought in 2018 caused widespread water shortages, hosepipe bans and challenges for grass growth in a pasture based agricultural system (Falzoi et al., 2019).

While no other studies to date have evaluated changes in future drought in Ireland, studies of observational records have revealed trends toward increasing summer drought magnitude. O'Connor, Murphy, Matthews, and Wilby (2022) and O'Connor, Meresa, and Murphy (2022) examined trends in summer drought for reconstructions of SPI and SSI spanning 1900 to present, finding trends toward shorter, more intense meteorological and hydrological droughts. Similarly, Vicente-Serrano et al. (2020b) examined long term variability and change in meteorological droughts in western Europe using quality assured precipitation series, finding that trends toward increased drought magnitude in Ireland were among the largest trends identified in Europe. Both studies also found decreasing trends in drought on an annual basis, consistent with projected changes found here.

Despite large increases in summer moisture deficits, analysis of the duration and frequency of drought events revealed large uncertainties. This is likely due to changes outside of summer season with wetter winters and spring offsetting increases in duration and frequency in summer months. While the direction of change in individual drought characteristics is uncertain, the ensemble mean changes by the 2080s signal increased duration of meteorological droughts (SPI-3 and SPEI-3) along with increased duration of groundwater drought (SBI-3). Largest increases in the latter are found for catchments with low groundwater storage. For catchments with high groundwater storage, the ensemble mean indicates decreased drought duration, likely because of increases of winter and spring precipitation. These findings highlight the susceptibility to multi-year droughts, whereby a dry winter/spring increases the risk of extreme droughts given the large scale summer drying indicated by the ensemble mean (Browne et al., 2016; Van der Wiel et al., 2022).

Changes in drought propagation were investigated using ensemble mean projections. The time lag showing maximum correlation between meteorological and hydrological drought was found to increase by up to 2 months by the 2080s. This is consistent with increases in precipitation resulting in additional storage in catchments, with the greatest increases in lag times evident for catchments with greater storage capacity. Modest changes in the propagation of meteorological to hydrological drought events were found for the 3-month accumulation period. For 12-accumulations, all catchments show an increase in propagation probability by mid-century, with some catchments showing a  $>10\%$  increase. Notably the probability of drought propagation from SPI to SBI are not as high for the 2080s, indicating the importance of increases in winter and spring precipitation in offsetting drought propagation to baseflow. A similar finding was reported for UK catchments by Parry et al. (2023) whereby changes in drought were more modest for groundwater relative to runoff. They also highlight more modest changes by the end of century relative to mid-century using an independent set of climate scenarios and hydrological models. As we do here, Parry et al. (2023) highlight



the role of wetter winters toward the end of the century as a key driver of this finding. Increases in the probability of drought propagation have been found in other contexts (e.g., Jehanzaib et al., 2020 in South Korea).

There are several limitations to note. We evaluated five bias correction techniques finding DGQM best suited for our purposes. However, no bias correction technique is perfect, and performance is different across catchments and drought accumulation periods. DGQM performed best for the 3-month accumulation period, while EQM performed marginally better for longer accumulation periods (6- and 12-month). Bias correction also tended to have the greatest impact on drought magnitude, with DGQM performing best in this regard. Therefore, future work should examine the sensitivity of our results to bias correction techniques employed. While uncertainty ranges in projected changes are large, they are likely to be underestimated here, particularly for hydrological drought (SSI and SBI). We do not include uncertainty due to hydrological model structure which is likely to impact on the range of change simulated (Addor et al., 2014; Bastola et al., 2011; H. K. Meresa & Romanowicz, 2017). Future work should explore the sensitivity of results to different hydrological model structure, although we note that Parry et al. (2023) find overall consensus between four different hydrological model structures in terms of simulation of drought characteristics in the UK. Exploring model structural uncertainty is particularly important in assessing the role of baseflow contributions and the influence of increased precipitation in winter/spring seasons on drought magnitude, frequency and propagation in summer.

It is also important to note that the changes presented here assume no changes in landuse for future time periods. Landuse strategies to mitigate greenhouse gases, implemented on large scales, such as afforestation, are likely to influence drought risk. Some studies show that vegetation change, through partitioning of green and blue water, can have significant implications for hydrological drought risk (e.g., Mastrotheodoros et al., 2020; Peña-Angulo et al., 2022; Vicente-Serrano et al., 2021). Future research could examine scenarios of climate and landuse change and their combined impact on droughts at the catchment scale using physically based models capable of integrating such feedbacks.

## 5. Conclusions

This study examines changing drought characteristics and propagation under climate change for 10 Irish catchments. Twelve GCMs from the CMIP6 archive forced by SSP370, were bias corrected and used as input to a conceptual hydrological model. Standardized drought indices for different accumulation periods were fitted to simulated precipitation (SPI), moisture deficits (SPEI), streamflow (SSI) and baseflow (SBI). Drought characteristics, including the magnitude, frequency and duration were evaluated seasonally and for individual events for each future time period, and the changing probability of propagation from meteorological to hydrological events was assessed. Our results indicate substantial drying during summer with associated increases in summer drought magnitude and frequency. However, simulations show a wide range of change, especially for SSI and SBI. Only modest changes in the magnitude and frequency of drought events were found outside of summer, with increases in winter and spring precipitation offsetting summer dryness. Large uncertainties mean that even the direction of change in the duration and frequency of drought events is unclear. Finally, we find an increase in the probability of drought propagation from meteorological to hydrological events for catchments where groundwater storage is limited. For catchments with ample groundwater storage, decreases in drought propagation were evident for the 2080s, again likely driven by increases in precipitation outside of summer. As the first analysis to investigate future drought risk in Ireland at the catchment scale, using multiple indices, these findings should inform adaptation planning.

## Conflict of Interest

The authors declare no conflicts of interest relevant to this study.

## Data Availability Statement

All hydrological, meteorological, and physiographic data used in this research study are publicly available online at their respective organizational website at no charge fee and with unrestricted access. The climate change dataset of CMIP6 climate models are available at <https://esgf-node.llnl.gov/search/cmip6/>. The observed Irish meteorological data are available at <https://www.met.ie/climate/available-data>. The observed streamflow data are available at <https://waterlevel.ie/hydro-data/>. Full analyses were implemented and done, and figures were made with Matlab software from Matlab official website ([https://fr.mathworks.com/pricing-licensing.html?intenduse=comm&s\\_tid=htb\\_learn\\_gtwy\\_cta1](https://fr.mathworks.com/pricing-licensing.html?intenduse=comm&s_tid=htb_learn_gtwy_cta1)) licensed to Hadush Meresa at Maynooth University.

## Acknowledgments

We acknowledge, with thanks, Met Éireann, The Office of Public Works (OPW) and The Environmental Protection Agency (EPA) for the provision of data. This research was by the Irish Environmental Protection Agency (EPA) Grant/Award Number 2018-CCRP-MS.51: HydroPredict-Ensemble Riverflow Scenarios for Climate Change Adaptation. CM and SD also acknowledge funding from Science Foundation Ireland Grant/Award Number: SFI/17/CDA/4783. Open access funding provided by IReL.

## References

- Addor, N., Rössler, O., Köplin, N., Huss, M., Weingartner, R., & Seibert, J. (2014). Robust changes and sources of uncertainty in the projected hydrological regimes of Swiss catchments. *Water Resources Research*, *50*(10), 7541–7562. <https://doi.org/10.1002/2014wr015549>
- Apurv, T., Sivapalan, M., & Cai, X. (2017). Understanding the role of climate characteristics in drought propagation. *Water Resources Research*, *53*(11), 9304–9329. <https://doi.org/10.1002/2017wr021445>
- Ayantobo, O. O., Li, Y., Song, S., & Yao, N. (2017). Spatial comparability of drought characteristics and related return periods in Mainland China over 1961–2013. *Journal of Hydrology*, *550*, 549–567. <https://doi.org/10.1016/j.jhydrol.2017.05.019>
- Barker, L. J., Hannaford, J., Chiverton, A., & Svensson, C. (2016). From meteorological to hydrological drought using standardised indicators. *HESS*, *20*(6), 2483–2505. <https://doi.org/10.5194/hess-20-2483-2016>
- Bastola, S., Murphy, C., & Sweeney, J. (2011). The role of hydrological modelling uncertainties in climate change impact assessments of Irish river catchments. *Advances in Water Resources*, *34*(5), 562–576. <https://doi.org/10.1016/j.advwatres.2011.01.008>
- Bosch, D. D., Arnold, J. G., Allen, P. G., Lim, K., & Shik, Y. (2017). Journal of hydrology: Regional studies temporal variations in baseflow for the little river experimental watershed in South Georgia, USA. *Biochemical Pharmacology*, *10*, 110–121. <https://doi.org/10.1016/j.ejrh.2017.02.002>
- Browne, A. L., Dury, S., & de Boer, C. (2016). Isabelle la. and Stein, Ulf. Governing for Drought and Water Scarcity in the Context of Flood Disaster Recovery: The Curious Case of Somerset, United Kingdom. In H. Bressers, N. Bressers, & C. Larrue (Eds.), *Governance for drought resilience*. [https://doi.org/10.1007/978-3-319-29671-5\\_5](https://doi.org/10.1007/978-3-319-29671-5_5)
- Eckhardt, E. (2008). A comparison of baseflow indices, which were calculated with seven different baseflow separation methods [software]. *Journal of Hydrology*, *352* (1–2), 168–173. <https://doi.org/10.1016/J.JHYDROL.2008.01.005>
- Eltahir, E. A. B., & Yeh, P. J. F. (1999). On the asymmetric response of aquifer water level to floods and droughts in Illinois. *Water Resources Research*, *35*(4), 1199–1217. <https://doi.org/10.1029/1998wr900071>
- Eyring, V., Bony, S., Meehl, G. A., Senior, C. A., Stevens, B., Stouffer, R. J., & Taylor, K. E. (2016). Overview of the coupled model Inter-comparison project phase 6 (CMIP6) experimental design and organization. *Geoscientific Model Development*, *9*(5), 1937–1958. <https://doi.org/10.5194/gmd-9-1937-2016>
- Falzo, S., Gleeson, E., Lambkin, K., Zimmermann, J., Marwaha, R., O'Hara, R., et al. (2019). Analysis of the severe drought in Ireland in 2018. *Weather*, *74*(11), 368–373. <https://doi.org/10.1002/wea.3587>
- Funk, C., Harrison, L., Alexander, L., Peterson, P., Behrangi, A., & Husak, G. (2019). Exploring trends in wet-season precipitation and drought indices in wet, humid and dry regions.
- Gaitán, E., Monjo, R., Pórtoles, J., & Pino-otín, M. R. (2020). Science of the total environment impact of climate change on drought in Aragon (NE Spain). *Science of the Total Environment*, *740*(June), 140094. <https://doi.org/10.1016/j.scitotenv.2020.140094>
- Ganguli, P., Singh, B., Reddy, N. N., Raut, A., Mishra, D., & Das, B. S. (2022). Climate-catchment-soil control on hydrological droughts in peninsular India. *Scientific Reports*, *12*(1), 8014. <https://doi.org/10.1038/s41598-022-11293-7>
- Golian, S., & Murphy, C. (2021). Evaluation of sub-selection methods for assessing climate change impacts on low-flow and hydrological drought conditions. *Water Resources Management*, *35*(1), 113–133. <https://doi.org/10.1007/s11269-020-02714-1>
- Hallouin, T., Bruen, M., & Loughlin, F. E. O. (2020). Calibration of hydrological models for ecologically relevant streamflow predictions: A trade-off between fitting well to data and estimating consistent parameter sets? *Hydrology and Earth System Sciences*, *1997*(3), 1031–1054. <https://doi.org/10.5194/hess-24-1031-2020>
- Hanel, M., Rakovec, O., Markonis, Y., Máca, P., Samaniego, L., Kysely, J., & Kumar, R. (2018). Revisiting the recent European droughts from a long-term perspective. <https://doi.org/10.1038/s41598-018-27464-4>
- Hänsel, S., Ustrnul, Z., Lupikasza, E., & Skalak, P. (2019). Assessing seasonal drought variations and trends over Central Europe. *Advances in Water Resources*, *127*, 53–75. <https://doi.org/10.1016/j.advwatres.2019.03.005>
- Hao, Z., & Aghakouchak, A. (2013). Advances in water resources multivariate standardized drought index: A parametric multi-index model. *Advances in Water Resources*, *57*, 12–18. <https://doi.org/10.1016/j.advwatres.2013.03.009>
- He, Z., Unger-shayesteh, K., Vorogushyn, S., Weise, S. M., & Duethmann, D. (2019). Comparing Bayesian and traditional end-member mixing approaches for hydrograph separation in a glacierized basin.
- Intergovernmental Panel on Climate Change (IPCC). (2021). *Earth and environmental sciences, climatology and climate change, environmental policy, economics and law*. Cambridge University Press. <https://doi.org/10.1017/CBO9781107415324>
- Ionita, M., Tallaksen, L. M., Kingston, D. G., Stage, J. H., Laaha, G., Lanen, H. A. J. V., et al. (2017). The European 2015 drought from a climatological perspective. *Hydrology and Earth System Sciences*, *21*(3), 1397–1419. <https://doi.org/10.5194/hess-21-1397-2017>
- Jehanzaib, M., Sattar, M. N., Lee, J. H., & Kim, T. W. (2020). Investigating effect of climate change on drought propagation from meteorological to hydrological drought using multi-model ensemble projections. *Stochastic Environmental Research and Risk Assessment*, *34*(1), 7–21. <https://doi.org/10.1007/s00477-019-01760-5>
- Kirono, D. G. C., Round, V., Heady, C., Chiew, F. H. S., & Osbrough, S. (2020). Drought projections for Australia: Updated results and analysis of model simulations. *Weather and Climate Extremes*, *30*, 100280. <https://doi.org/10.1016/j.wace.2020.100280>
- Mann, M. E., & Gleick, P. H. (2015). Climate change and California drought in the 21st century. *Proceedings of the National Academy of Sciences*, *112*(13), 3858–3859. <https://doi.org/10.1073/pnas.1503667112>
- Mastrotheodoros, T., Pappas, C., Molnar, P., Burlando, P., Manoli, G., Parajka, J., et al. (2020). More green and less blue water in the Alps during warmer summers. *Nature Climate Change*, *10*(2), 155–161. <https://doi.org/10.1038/s41558-019-0676-5>
- McKee, T. B., Doesken, N. J., & Kleist, J. (1993). The relationship of drought frequency and duration to time scales. January, 17–22.
- Meresa, H., Donegan, S., Golian, S., & Murphy, C. (2022). Simulated changes in seasonal and low flows with climate change for Irish catchments. *Water*, *14*(10), 1556. <https://doi.org/10.3390/w14101556>
- Meresa, H., Murphy, C., Fealy, R., & Golian, S. (2021). Uncertainties and their interaction in flood hazard assessment with climate change. *Hydrology and Earth System Sciences*, *25*(9), 5237–5257. <https://doi.org/10.5194/hess-25-5237-2021>
- Meresa, H., & Zhang, Y. (2021). Contrasting uncertainties in estimating floods and low flow extremes. *Water Resources Management*, *35*(6), 1775–1795. <https://doi.org/10.1007/s11269-021-02809-3>
- Meresa, H. K., Osuch, M., & Romanowicz, R. (2016). Hydro-meteorological drought projections into the 21-st century for selected polish catchments. *Water (Switzerland)*, *8*(5), 206. <https://doi.org/10.3390/w8050206>
- Meresa, H. K., & Romanowicz, R. J. (2017). The critical role of uncertainty in projections of hydrological extremes. *Hydrology and Earth System Sciences*, *21*(8), 4245–4258. <https://doi.org/10.5194/hess-21-4245-2017>

- Mishra, V., & Cherkauer, K. A. (2010). Agricultural and forest meteorology retrospective droughts in the crop growing season: Implications to corn and soybean yield in the Midwestern United States. *Agricultural and Forest Meteorology*, *150*(7–8), 1030–1045. <https://doi.org/10.1016/j.agrformet.2010.04.002>
- Mockler, E. M., O'Loughlin, F. E., & Bruen, M. (2016). Understanding hydrological flow paths in conceptual catchment models using uncertainty and sensitivity analysis [software]. *Computers & Geosciences*, *90*, 66–77. <https://doi.org/10.1016/j.cageo.2015.08.015>
- Mukherjee, S., Mishra, A., & Trenberth, K. E. (2018). Climate change and drought: A perspective on drought indices. *Current Climate Change Reports*, *4*(2), 145–163. <https://doi.org/10.1007/s40641-018-0098-x>
- Murphy, A. (1988). Skill scores based on the mean square error and their relationships to the correlation coefficient [software]. *Monthly Weather Review*, *116*(12), 2417–2424. [https://doi.org/10.1175/1520-0493\(1988\)116<2417:ssbotm>2.0.co;2](https://doi.org/10.1175/1520-0493(1988)116<2417:ssbotm>2.0.co;2)
- Murphy, C., Broderick, C., Burt, T. P., Curley, M., Duffy, C., Hall, J., et al. (2018). A 305-year continuous monthly rainfall series for the island of Ireland (1711–2016). *Climate of the Past*, *14*(3), 413–440. <https://doi.org/10.5194/cp-14-413-2018>
- Murphy, C., Fealy, R., Charlton, R., & Sweeney, J. (2006). The reliability of an “off-the-shelf” conceptual rainfall runoff model for use in climate impact assessment: Uncertainty quantification using Latin hypercube sampling. *Area*, *38*(1), 65–78. <https://doi.org/10.1111/j.1475-4762.2006.00656.x>
- Murphy, C., Kettle, A., Meresa, H., Golian, S., Bruen, M., O'Loughlin, F., & Mellander, P. E. (2023). Climate change impacts on Irish river flows: High resolution scenarios and comparison with CORDEX and CMIP6 ensembles. *Water Resources Management*, *37*(5), 1841–1858. <https://doi.org/10.1007/s11269-023-03458-4>
- Murphy, C., Wilby, R. L., Matthews, T., Horvath, C., Crampsie, A., Ludlow, F., et al. (2020). The forgotten drought of 1765–1768: Reconstructing and re-evaluating historical droughts in the British and Irish Isles. *Journal of Climatology*, *40*(12), 5329–5351. <https://doi.org/10.1002/joc.6521>
- Nash, J. E., & Sutcliffe, J. V. (1970). River Flow forecasting through conceptual model. Part I—A discussion of principles. *Journal of Hydrology*, *10*(3), 282–290. [https://doi.org/10.1016/0022-1694\(70\)90255-6](https://doi.org/10.1016/0022-1694(70)90255-6)
- Niemeyer, S. (2008). New drought indices (Vol. 274, pp. 267–274).
- Nolan, P., O'sullivan, J., & Mcgrath, R. (2017). Impacts of climate change on mid-twenty-first century rainfall in Ireland: A high-resolution regional climate model ensemble approach. *International Journal of Climatology*, *37*(12), 4347–4363. <https://doi.org/10.1002/joc.5091>
- Noone, S., Broderick, C., Duffy, C., Matthews, T., Wilby, R. L., & Murphy, C. (2017). A 250-year drought catalogue for the island of Ireland (1765–2015). *International Journal of Climatology*, *37*, 239–254. <https://doi.org/10.1002/joc.4999>
- O'Connor, P., Meresa, H., & Murphy, C. (2022). Trends in reconstructed monthly, seasonal and annual flows for Irish catchments (1900–2016). *Weather*, 1477–8696. <https://doi.org/10.1002/wea.4288>
- O'Connor, P., Murphy, C., Matthews, T., & Wilby, R. L. (2022). Historical droughts in Irish catchments 1767–2016. *International Journal of Climatology*, *36*(3), 1299–1312. <https://doi.org/10.1002/joc.4425>
- Oguntunde, P. G., Lischeid, G., & Abiodun, B. J. (2017). Impacts of climate variability and change on drought characteristics in the Niger River Basin, West Africa. *Stochastic Environmental Research and Risk Assessment*, *32*(4), 1017–1034. <https://doi.org/10.1007/s00477-017-1484-y>
- Oudin, L., Hervieu, F., Michel, C., Perrin, C., Andréassian, V., Anctil, F., & Loumagne, C. (2005). Which potential evapotranspiration input for a lumped rainfall–runoff model? Part 2—Towards a simple and efficient potential evapotranspiration model for rainfall–runoff modelling. *Journal of Hydrology*, *303*(1–4), 290–306. <https://doi.org/10.1016/j.jhydrol.2004.08.026>
- Palmer, W. C. (1965). Meteorological drought. In *Research paper, 45, U.S. Weather Bureau, Washington, D.C.* (p. 58).
- Parry, S., Mackay, J. D., Chitson, T., Hannaford, J., Bell, V. A., Facer-Childs, K., et al. (2023). Divergent future drought projections in UK river flows and groundwater levels. *Hydrology and Earth System Sciences Discussions*. <https://doi.org/10.5194/hess-2023-59>
- Peña-Angulo, D., Vicente-Serrano, S. M., Domínguez-Castro, F., Lorenzo-Lacruz, J., Murphy, C., Hannaford, J., et al. (2022). The complex and spatially diverse patterns of hydrological droughts across Europe. *Water Resources Research*, *58*(4), e2022WR031976. <https://doi.org/10.1029/2022wr031976>
- Pontes Filho, J. D., Portela, M. M., Marinho de Carvalho Studart, T., & Souza Filho, F. D. A. (2019). A continuous drought probability monitoring system, CDPMS, based on copulas. *Water*, *11*(9), 1925. <https://doi.org/10.3390/w11091925>
- Quevauviller, P., & Gemmer, M. (2015). ScienceDirect EU and international policies for hydrometeorological risks: Operational aspects and link to climate action. *Advances in Climate Change Research*, *6*(1), 74–79. <https://doi.org/10.1016/j.accre.2015.09.002>
- Reyniers, N., Osborn, T. J., Addor, N., & Darch, G. (2022). Projected changes in droughts and extreme droughts in Great Britain strongly influenced by the choice of drought index. *Hydrology and Earth System Sciences Discussions*. <https://doi.org/10.5194/hess-2022-94>
- Ribeiro, A. F. S., Russo, A., Gouveia, C. M., Páscoa, P., & Pires, C. A. L. (2019). Probabilistic modelling of the dependence between rainfed crops and drought hazard. *HESS*, *19*(12), 2795–2809. <https://doi.org/10.5194/hess-19-2795-2019>
- Romanowicz, R. J., Kundzewicz, Z. W., Meresa, H. K., Stoffel, M., Krysanova, V., & Doroszkiewicz, J. (2016). Projections of changes in flood Hazard in two headwater catchments of the Vistula in the context of European-scale studies. In Z. W. Kundzewicz, M. Stoffel, T. Niedźwiedz, & B. Wyźga (Eds.), *Flood risk in the upper Vistula basin* (pp. 341–359). Springer.
- Roudier, P., Andersson, J. C. M., Donnelly, C., Feyen, L., Greuell, W., & Ludwig, F. (2015). Projections of future floods and hydrological droughts in Europe under a +2°C global warming. *Climatic Change*, *135*(2), 341–355. <https://doi.org/10.1007/s10584-015-1570-4>
- Shah, J., Hari, V., Rakovec, O., Markonis, Y., Samaniego, L., Mishra, V., et al. (2022). Increasing footprint of climate warming on flash droughts occurrence in Europe. *Environmental Research Letters*, *17*, 064017. <https://doi.org/10.1088/1748-9326/ac6888>
- Shin, J. Y., Chen, S., Lee, J.-H., & Kim, T.-W. (2018). Investigation of drought propagation in South Korea using drought index and conditional probability. *Terrestrial, Atmospheric and Oceanic Sciences*, *29*(2), 231–241. <https://doi.org/10.3319/tao.2017.08.23.01>
- Shukla, S., & Wood, A. W. (2008). Use of a standardized runoff index for characterizing hydrologic drought. *Geophysical Research Letters*, *35*(2), L02405. <https://doi.org/10.1029/2007GL032487>
- Spinoni, J., Vogt, J. V., Naumann, G., Barbosa, P., & Dosio, A. (2018). Will drought events become more frequent and severe in Europe? *International Journal of Climatology*, *38*(4), 1718–1736. <https://doi.org/10.1002/joc.5291>
- Stagge, J. H., Tallaksen, L. M., Gudmundsson, L., Loon, F. V., & Stahl, K. (2015). Candidate distributions for climatological drought indices (SPI and SPEI). *International Journal of Climatology*, *35*(13), 4027–4040. <https://doi.org/10.1002/joc.4267>
- Sutanto, S. J., & Van Lanen, H. A. J. (2022). Catchment memory explains hydrological drought forecast performance. *Scientific Reports*, *12*(1), 2689. <https://doi.org/10.1038/s41598-022-06553-5>
- Teutschbein, C., & Seibert, J. (2013). Is bias correction of regional climate model (RCM) simulations possible for non-stationary conditions. *Hydrology and Earth System Sciences*, *17*(12), 5061–5077. <https://doi.org/10.5194/hess-17-5061-2013>
- Tsakiris, G., & Vangelis, H. (2005). Establishing a drought index incorporating evapotranspiration (pp. 3–11).
- Ullrich, P., Xu, Z., Rhoades, A., Dettinger, M., Mount, J., Jones, A., & Vahmani, P. (2018). California's drought of the future: A midcentury recreation of the exceptional conditions of 2012–2017. *Earth's Future*, *6*(11), 1568–1587. <https://doi.org/10.1029/2018ef001007>

- Van der Wiel, K., Batelaan, T. J., & Wanders, N. (2022). Large increases of multi-year droughts in north-western Europe in a warmer climate. *Climate Dynamics*, *60*(5–6), 1781–1800. <https://doi.org/10.1007/s00382-022-06373-3>
- Vicente-Serrano, S. M., Domínguez-Castro, F., McVicar, T. R., Tomas-Burguera, M., Peña-Gallardo, M., Noguera, I., et al. (2020a). Global characterization of hydrological and meteorological droughts under future climate change: The importance of timescales, vegetation-CO<sub>2</sub> feedbacks and changes to distribution functions. *International Journal of Climatology*, *40*(5), 2557–2567. <https://doi.org/10.1002/joc.6350>
- Vicente-Serrano, S. M., Domínguez-Castro, F., Murphy, C., Hannaford, J., Reig, F., Peña-Angulo, D., et al. (2020b). Long-term variability and trends in meteorological droughts in Western Europe (1851–2018). *International Journal of Climatology*, *41*(S1), 1–28. <https://doi.org/10.1002/joc.6719>
- Vicente-Serrano, S. M., Domínguez-Castro, F., Murphy, C., Peña-Angulo, D., Tomas-Burguera, M., Noguera, I., et al. (2021). Increased vegetation in mountainous headwaters amplifies water stress during dry periods. *Geophysical Research Letters*, *48*(18), e2021GL094672. <https://doi.org/10.1029/2021gl094672>
- Vicente-Serrano, S. M., SergioBeguiría, M., López-Moreno, J. I., López-Moreno, & Juan, I. (2010). A multiscalar drought index sensitive to global warming: The standardized precipitation evapotranspiration index. *Journal of Climate*, *23*(7), 1696–1718. <https://doi.org/10.1175/2009JCLI2909.1>
- Wossenyeleh, B. K., Worku, K. A., Verbeiren, B., & Huysmans, M. (2021). Drought propagation and its impact on groundwater hydrology of wetlands: A case study on the Doode Bemde nature reserve (Belgium). *Natural Hazards and Earth System Sciences*, *21*(1), 39–51. <https://doi.org/10.5194/nhess-21-39-2021>
- Zhou, Z., Shi, H., Fu, Q., Ding, Y., Li, T., & Liu, S. (2021). Investigating the propagation from meteorological to hydrological drought by introducing the nonlinear dependence with directed information transfer index. *Water Resources Research*, *57*(8), e2021WR030028. <https://doi.org/10.1029/2021WR030028>